Modeling of twisted and coiled polymer (TCP) muscle based on phenomenological approach

IOP Publishing Smart Materials and Structures
Smart Mater. Struct. **26** (2017) 125010 (12pp) https://doi.org/10.1088/1361-665X/aa8d7d

Modeling of twisted and coiled polymer (TCP) muscle based on phenomenological approach

Farzad Karami and Yonas Tadesse

Humanoid, Biorobotics and Smart Systems (HBS) Laboratory, Department of Mechanical Engineering, The University of Texas at Dallas, Richardson, Texas-75080, United States of America

E-mail: yonas.tadesse@utdallas.edu

Received 15 June 2017, revised 8 September 2017
Accepted for publication 19 September 2017
Published 2 November 2017

Abstract

Twisted and coiled polymers (TCP) muscles are linear actuators that respond to change in temperature. Exploiting high negative coefficient of thermal expansion (CTE) and helical geometry give them a significant ability to change length in a limited temperature range. Several applications and experimental data of these materials have been demonstrated in the last few years. To use these actuators in robotics and control system applications, a mathematical model for predicting their behavior is essential. In this work, a practical and accurate phenomenological model for estimating the displacement of TCP muscles, as a function of the load as well as input electrical current, is proposed. The problem is broken down into two parts, i.e. modeling of the electro-thermal and then the thermo-elastic behavior of the muscles. For the first part, a differential equation, with changing electrical resistance term, is derived. Next, by using a temperature-dependent modulus of elasticity and CTE as well as taking the geometry of the muscles into account, an expression for displacement is derived. Experimental data for different loads and actuation current levels are used for verifying the model and investigating its accuracy. The result shows a good agreement between the simulation and experimental results for all loads.

Keywords: phenomenological modeling, smart materials, actuators, artificial muscles, lumped parameter

(Some figures may appear in colour only in the online journal)

1. Introduction

The use of thermal actuation for creating desired motion has a long history. It is the most simple and easy to use method for making displacement in mechanisms, but the low coefficient of thermal expansion limits this method to applications with small displacement. This value ranges from near zero for some alloys, such as Sitall, to large values for specific types of polymers. Even for a material with a large CTE, the expected linear displacement cannot exceed few millimeters in an allowable temperature range of the chosen material. The convenience of using thermal actuation has motivated researchers to work on finding materials with a higher response to heating, with higher CTEs, or proposing modifications in geometry to magnify the limited thermal displacement into a large motion. To have high actuation, several types of materials with a high CTE have been developed and tested. The alternative method, i.e. using an amplifying geometry, is proven to be less expensive and easier to achieve. Using the alternative geometries, instead of a single straight actuator, a wound structure adds to the possible stroke. The most well-known of such configurations is helix which shows significant stroke with an equal load as compared with a single rod under axial load. Using polymers, instead of metal wire, as the precursor fiber in a helical spring and exploiting a large negative CTE of polymers, which is magnified by the helical geometry, is the cornerstone of a newly proposed actuator called TCP muscles [1–5]. Due to an

increase in the actual length of the fiber and also reducing the effective stiffness of a TCP muscle, it can exhibit a considerably larger displacement in response to heating. These muscles are heated up by electric current sent through conductive precursor fibers used in the preparation of the muscle or using a liquid flow to flow over the muscle for heating and cooling. The TCP actuator can be used in many applications where low cost, ease of use, compact size, and low weight are necessary. These qualities, make TCP muscles a very good choice for light weight and economic robots [6, 7]. It also has found popularity in actuation of humanoid robots [8] and a soft robot or morphing structures [9], multilayer robot skin [10], tensegrity robot [11], orthotic hand [7, 12], prosthetic hand [13], musculoskeletal system [14, 15] demonstrated from our group. These show that the actuators are easy to use for practical applications. The coiled form has been shown to be effective with shape memory alloys (SMA). Using SMAs in a helical form can significantly increase the linear displacement comparing with a wire form of SMA of the same length [16].

To use these newly proposed artificial muscles in applications which need length control, it is necessary to derive a mathematical model to link the input electric signal to the output displacement or force. This model should describe the thermomechanical behavior of a TCP muscle to give a prediction of the length based on geometry, temperature, and load. The modeling problem can be broken down into two disciplines: thermal and mechanical. The thermal aspect of modeling concerns with finding a relation between the electrical actuation and the rise and fall in temperature of a TCP muscle. There are different physics taking roles in this phenomenon, such as the electrical behavior of the conductive part, and heat transfer between members inside muscles and the surrounding environment. The electrical resistance and its effect on the overall performance of TCP muscles are not investigated so far. The heat transfer mechanism consists of conductive heat flow through the muscle, convective heat transfer between the muscle and the surrounding medium, and energy exchange via radiation. Among the possible heat transfer mechanisms, the convection heat transfer is the matter of interest and the others have fewer effects on the actual thermal behavior of the muscle. Due to stretching of the heat source, the conductor inside the muscle elongates along the length of muscles and negligible dimensions in thickness, the conductive heat transfer contribution would be negligible. On the other hand, radiation dominates the heat transferring in high temperature, e.g. higher than 1000 °C, and it can be ignored in room condition at which muscles are used. Similar assumptions were taken in modeling related composite actuators [17].

The actuation method used in this work is based on Joule heating (electro-thermal) of the muscle via passing electrical current through a conductive fiber woven among polymer fibers. The resistance of the conductive material, commonly made by metal, causes an energy conversion from electrical to heat. This heat would raise the temperature of the muscle with respect to boundary conditions. Heating up of metals causes an increase in the electrical resistance and, consequently, an increase in the amount of heat generated. Polymers are sensitive to temperature, so heating changes the mechanical properties significantly. Given that TCP muscles are mainly made of polymers, it is necessary to investigate the change in characteristics, during the actuation process, to make any modeling more reliable. There is much research for every type of polymers and their characteristics in different temperature levels. There are also related works dedicated to developing a quantified model for temperature dependent characteristics of polymers [1, 18, 19].

Regarding modeling of TCPs, a modified spring-mass linear model system has been used to express the behavior of TCP muscles [20]. There are some other works focusing on the mechanical behavior of these actuators. In [21], a top-down approach is exploited to find a relation between microscopic properties of the material and macroscopic behavior of TCP muscles. In this work, the authors focused on the static and steady-state behavior. In the other work, a statistical thermodynamics approach is used to explain the change in the structure of the polymers with respect to the temperature [22]. They proposed that mechanical characteristics are a function of the volume ratio of different phases inside the polymer structure. They also adopted the normal distribution to predict the phase conversion by taking the temperature as a random variable, and for mechanical part, linear model of helical springs was used. In [23], a kinematic relationship between the elastic constants of the material and the twisted member is proposed and the effect of geometry, as the helix angle of muscles, on the elastic behavior of the muscle is investigated. The dynamic behavior of the TCP muscles is investigated briefly so far [20, 24]. Yip and Niemeyer [20] have proposed a linear invariant first order model of TCP muscles and implemented it for a control application using a mass-spring-damper system. In their work, they consider the TCP muscles having constant characteristics over the temperature range. In the other work, Arakawa *et al* have used a black box model and system identification to obtain a dynamic model, regardless of the physical phenomena, to position control of a similar actuator [25]. Zhang *et al* proposed a model of hysteresis and a compensation method for TCP muscles [26].

There are some works focusing on heat transfer coefficients, mainly h as the convection heat transfer coefficient of TCP muscles and similar actuators. Research on finding the coefficients for the cylinders, wires, and rods, which are generally the shape of TCP muscles, is a well-established topic and there are many papers and book chapters dedicated to this topic [27]. The problem with using their results is that the shape of the TCP muscles is not an exact cylindrical wire and the closely packed helical shape makes a considerable deviation from smooth wires characteristics. Saharan and Tadesse studied the characteristics of TCP muscles and effect of different coiling speed on their performance focusing on 1-ply, 2-ply and 3-ply [28]. Another issue with TCP muscles is the speed of response to an actuation. These muscles are generally considered as slow actuators due to the slow cooling rate. To overcome this problem, some solutions are proposed

in the literature. This behavior is similar to SMAs, they need sufficient cooling time to return to the initial temperature. This cooling time can be reduced by active cooling methods, which in turn decrease the cooling time by increasing the convective heat transfer rate. For doing so, the first method is to use forced convection cooling method such as air or fluid flow over the muscle. The other proposition is to change the media in which muscle works. Haines *et al* [1] showed that a frequency of up to 7 Hz can be achieved by using helium gas to cool the actuators. In this paper, active cooling is not employed but such process will have influence in the convective heat transfer as was observed in similar actuators in SMAs [29]. The active cooling will have an effect on the convective heat transfer coefficient which will be discussed later in the paper.

The purpose of this work is to develop a model of TCP muscles' displacement through a phenomenological approach using a control volume. The effect of temperature on the electrical resistance of the conductor is modeled as a variable heat source and a modified differential equation for predicting the temperature rise is obtained. The parameters of the convective heat transfer are estimated by using a curve fitting on an experimental result and then applying to the rest of simulations. The model output and the test result are in a good agreement and accuracy of the electrical input current-temperature output model is assured. The displacement of the muscle is expressed as a function of temperature and load. The change in geometry, due to load, has been found to have a crucial effect on the behavior of the muscle. This effect is modeled by using a helical geometry, which is in accordance with the structure of TCP muscles. Two material properties have been identified to shape the response of the muscle to an actuation signal: CTE and modulus of elasticity which both are dependent on temperature. Then, expressions for both, as functions of temperature, are obtained and used in the model. For verifying the model, experimental data are used for different actuation levels. This data consists of the time history of displacement and temperature as well as actuating current. In this work, the hysteresis of the actuator is pointed out and an explanation is proposed.

2. Modeling

The behavior of TCP muscles can be investigated in two distinct yet related domain. The first one is the thermo-electrical part which consists of the heat transfer and electrical properties of the actuator. The second is the thermomechanical part that mostly explains how the actuator responds to the load in a certain temperature. These relationships are briefly shown in figure 1 as a block diagram.

We considered a scenario where the muscle is tested by a dead weight hung at one end and fixed at the other. This configuration can guarantee to have a constant load inside the actuator during the test. The muscle is exposed to still air in the absence of any forced air flow. The geometry of TCP muscle is a long string in longitude direction with negligible dimensions in the two others. Given that heat flux flows from the muscle

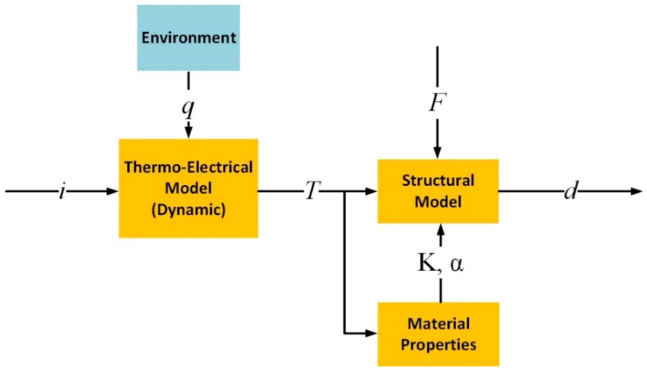

Figure 1. Block diagram of a TCP muscle model. (i is electrical current, T is temperature, q is heat flux, F is load, d is displacement, K is elastic modulus and α is CTE).

along the surface due to convection, and with an assumption of uniform resistance, heat flow due to conduction along the muscle can be neglected. On the other hand, the thickness of the muscle, in which the flux travels, is very small compared to its length. These lead to a small Biot number and validity of lumped parameter assumption, similar to the modeling of SMAs [29, 30]. Taking the length of the TCP muscle as control volume, the boundary conditions would be free convective heat transfer with the surrounding. There is also a heat generation by Joule heating inside the control volume. The overall thermo-electric configuration of a TCP muscle loaded with the dead weight at the end is shown in figure 2.

Using the first law of thermodynamics for the defined control volume, we have:

$$mc_p \frac{dT}{dt} = -hA(T - T_\infty) + i^2R \tag{1}$$

Where m is mass, c_p is the specific heat capacity, h is the coefficient of convection heat transfer, A is the area exposed to the ambient air, i is the electrical current provided to the muscle, T is the temperature in the muscle, T_∞ is the ambient temperature and R is the electrical resistance of the TCP muscle. The resistance of conductors is a function of material and geometry. It is defined as:

$$R = \rho \frac{l}{A} \tag{2}$$

In the above equation, ρ is the resistivity of the conductor, l is the length and A is the section area of the conductive part. It is well-known that the resistivity of the metals varies with temperature. Studies on the precursor fiber used for making the TCP muscles showed that the diameter of a typical fiber is 200 μm and the silver coating is 100 nm thick [31]. The step by step fabrication process of the silver coated TCP muscles are described in our recent work [6]. For metals, such as conductive fibers inside TCP muscles, the resistivity is modeled by a linear relation as follows:

$$\rho(T) = \rho_0(1 + \alpha(T - T_0)) \tag{3}$$

Where α is called temperature coefficient of resistivity, ρ_0 is resistivity in a reference temperature and T_0 is the reference temperature. Assuming a constant geometry, the resistance

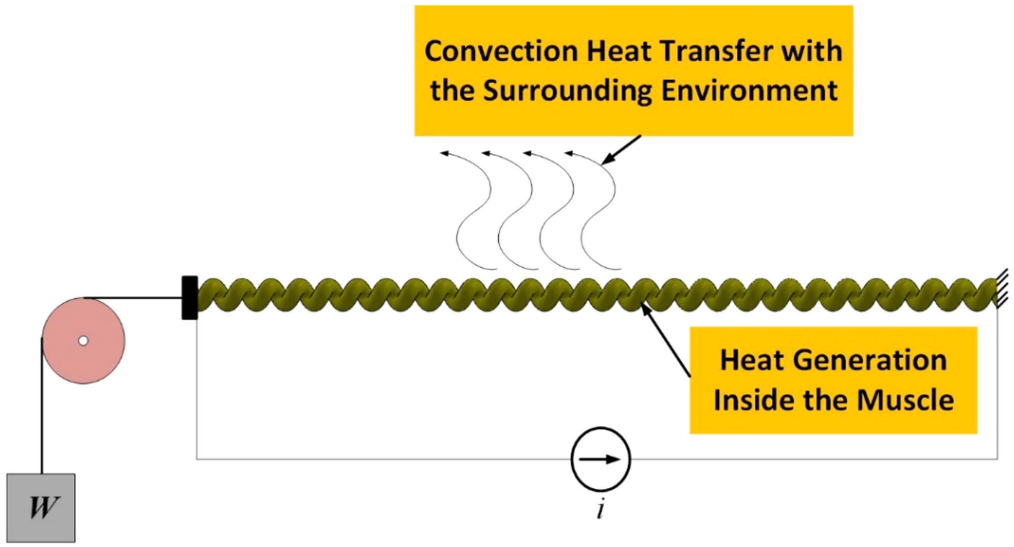

Figure 2. Configuration of a TCP muscle actuated by electricity, exposed to ambient air and subjected to an external load (W).

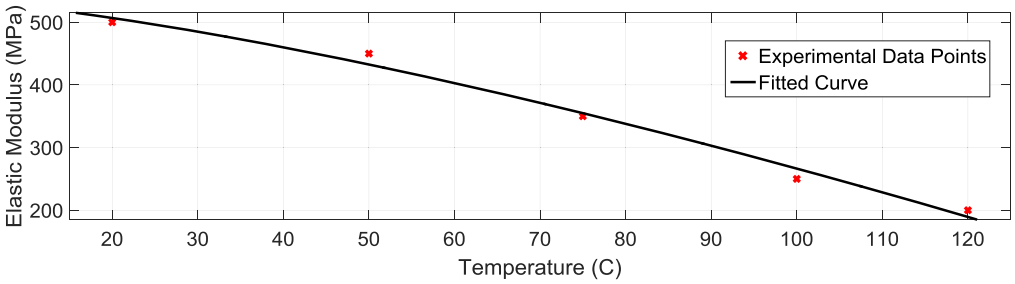

Figure 3. Elastic modulus of nylon 6/6 versus temperature [1].

equation can be rewritten in term of initial resistance and the change in resistance due to temperature by combining equations (1) and (3):

$$R(T) = R_0(1 + \alpha(T - T_0)) \tag{4}$$

Here R_o is the initial resistance of the muscle corresponding to equation (2). Substituting equation (4) in equation (1), one can write:

$$mc_p\frac{dT}{dt} = -hA(T - T_\infty) + i^2R_0(1 + \alpha(T - T_0)) \tag{5}$$

It is convenient to assume the same resistivity reference temperature T_0 and ambient temperature T_∞, so one can rearrange equation (5) to the following form:

$$mc_p\frac{d(T - T_\infty)}{dt} = (-hA + i^2R_0\alpha)(T - T_\infty) + i^2R_0 \tag{6}$$

The interesting result of the above equation is that if the magnitude of $i^2R_0\alpha$ is more than hA, then the differential equation will be unstable and the temperature rises constantly. The solution of the above equation for an initial temperature equal to ambient temperature is:

$$T - T_\infty = -\frac{R_0i^2}{-hA + R_0i^2\alpha}(1 - e^{\frac{-hA+R_0i^2\alpha}{mc_p}t}) \tag{7}$$

The elastic coefficients of nylon 6/6, which is commonly used as the precursor for TCP muscles, considerably depends on temperature. At high temperature, as experimental finding indicates, the elastic modulus of nylon 6/6 drops to a 50% of its value at room temperature. Granted that the displacement and force of a TCP muscle are related to the elastic modulus of its material, high temperature can change the performance of TCP muscles. Figure 3 shows the elastic modulus versus temperature. The figure is replicated from an experiment data by Haines *et al* [1].

The best-fitted function of the modulus E as a function of temperature T is obtained from the following form:

$$E(T) = a_1T^{a_2} + a_3 \tag{8}$$

Where a1, a2, and a3 are constants. According to the standard model of compression/extension springs, there is a linear dependency between the elastic coefficients of the material and the stiffness of a TCP muscle. The following equation shows this relation:

$$k = \frac{D^4G}{8d^3N} \tag{9}$$

Where D is the coil diameter, G is the shear modulus, d is the precursor fiber diameter and N is the number of coils. Using the relation between modulus of elasticity, modulus of shear and Poisson ratio for isotropic linear materials, the

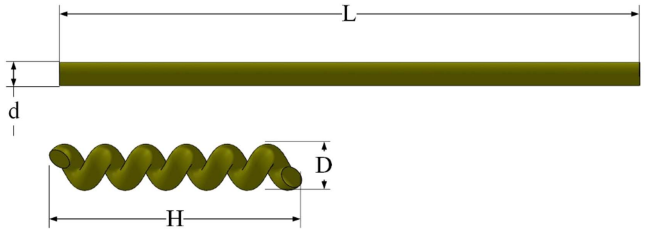

Figure 4. Geometry of a TCP muscle in coiled and uncoiled conditions (d is precursor diameter, D is coil diameter, L is precursor length, and H is coiled length).

equation (9) can be rewritten in the following form.

$$k = \frac{D^4}{8d^3N}\left(\frac{E}{2(1+\mu)}\right) \tag{10}$$

Where E is the elastic modulus and μ is the Poisson ratio of the material. Substituting the E from equation (8) into the equation (10) we have:

$$k = \frac{D^4}{8d^3N}\left(\frac{a_1 T^{a_2} + a_3}{2(1+\mu)}\right) \tag{11}$$

With the assumption of an unaltered geometry during the actuation, one can express the stiffness as a function of only temperature and convert the equation (11) to the following form:

$$k(T) = \gamma T^b \tag{12}$$

The γ coefficient, which represents all temperature-independent parameters, is obtained from a load-displacement test at room temperature. The elongation of the muscle due to a tension is obtained by:

$$\Delta_{el} = \frac{F}{k} \tag{13}$$

Where F is the load in the muscle. The experimental result of the testing the modeling approach and parameter values are presented in the simulation and experiment section. The main characteristic that made some materials suitable for use in a twisted and coiled configuration, as an actuator, is their high negative coefficient of thermal expansion. According to Harris [2], there is a temperature dependent relation between thermal expansion coefficient (CTE,α_T) and temperature in certain polymer materials such as liquid crystalline elastomeric actuators. Similar temperature dependence of thermal expansion coefficient of nylon 6,6 in the axial direction was described by Yang and Li [21]. We adopt a linear function of axial thermal expansion which is presented as:

$$\alpha_T = c_1 T + c_2 \tag{14}$$

This value can be used for calculation of contraction in a straight member, but, the change in the length of coiled muscles is different from the change of the precursor fibers defined by the linear thermal expansion equation. To find the change in height of TCP muscles, the geometry of the muscle should be taken into account. In figure 4, a description of a TCP muscle geometric parameters, used in this part of the study, is shown.

The height of the helix has the following relationship with diameter and length:

$$H = \sqrt{L^2 - \pi N^2 D^2} \tag{15}$$

Where, D and H are diameter and height of the helix, respectively, and L is the length of the precursor fiber. Assuming linear thermal expansion relation, by differentiating the equation (15) the following equation for the change in a TCP muscle height is obtained:

$$\Delta_{th} = \delta H = \frac{L\delta L}{\sqrt{L^2 - \pi D^2}} - \frac{\pi D \delta D}{\sqrt{L^2 - \pi D^2}} = \left(\frac{L_0^2}{H_0}\alpha_{\parallel}(T - T_0) - \frac{\pi D_0^2}{H_0}\alpha_{\perp}(T - T_0)\right) \tag{16}$$

Where $\alpha_{\parallel}$ is the CTE in longitudinal and $\alpha_{\perp}$ is the CTE in the transverse direction. Ignoring the negligible dimension of the muscle in thickness (radial axis), compared with its length, the second term of the above equation can be neglected. Since there is a reciprocal relationship between the initial height of the muscle and the overall displacement due to thermal contraction, as the initial length increases the total achievable thermal displacement will decrease. The subscript in each parameter H_0, L_0 and T_0 indicate the initial values of the corresponding parameters.

We are considering the homochiral TCP actuators that contract in response to heat in this modeling and analysis. The whole change in the length of the actuator can be considered as having two separate contrasting components. One is the elongation due to the load and the second is contraction caused by heating. These two components, with an assumption of unchanged geometry during actuation, can be added independently to give the total displacement of the muscle, as it follows:

$$\Delta H = H_0 - \Delta_{th} + \Delta_{el} \tag{17}$$

Which, Δ_{th} is thermal displacement and Δ_{el} is elastic displacement due to tension. Substituting the thermal displacement from the equation (16) and the linear spring model from the equation (11) into the equation (17) yields:

$$\Delta H(T) = H_0 - \left(\frac{L_0^2}{H_0} - \frac{\pi D_0^2}{H_0}\right)(c_1 T + c_2)(T - T_0) + \frac{D^4}{8d^3N}\left(\frac{aT^b}{2(1+\mu)}\right)F \tag{18}$$

This is an algebraic equation giving the displacement as a function of temperature and load. Along with the differential equation in the equation (6), this equation can give a prediction of displacement as a function of input actuation (electric current) and load.

High loads cause large deformation and consequently a deviation in the actual stiffness from the value predicted by the equation (13). The reason is a significant increase in the helix angle that makes the assumption of pure torsion no more valid. To take the effect of this phenomenon into the formulation, one can use the energy method with axial, torsional and shear terms as well [32]. The geometry of load

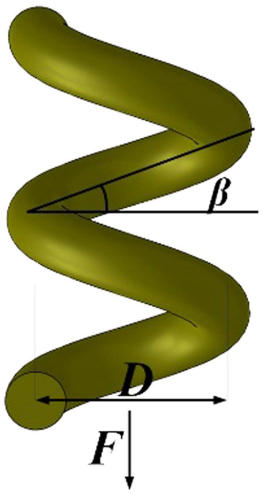

Figure 5. Geometry of load applied on a TCP muscle.

on a TCP muscle as a helical spring is shown in figure 5. It yields:

$$U = \int_0^L \left(\frac{F^2 \sin^2 \beta}{2EA} + \frac{F^2 \cos^2 \beta}{2GA} + \frac{R^2 F^2 \cos^2 \beta}{2GJ} \right) dx \quad (19)$$

Where U is the term for total elastic energy, β is the helix angle, A is the cross-section of the precursor, J is the polar moment of the precursor section, and R is the radius of the coil. In writing the above equation, given that the supports of TCP muscle allow free rotation around the longitudinal axis, it is assumed that there is no torsional torque applied to the muscle. Using Castigliano's theorem, the deflection due to F can be found by the following relation:

$$\delta = \frac{\partial U}{\partial F} = \int_0^L \left(\frac{F \sin^2 \beta}{EA} + \frac{F \cos^2 \beta}{GA} + \frac{R^2 F \cos^2 \beta}{GJ} \right) dx \quad (20)$$

During the actuation, the number of the coils and length of the precursor fiber remain constant and the diameter and height change according to the applied load. From the geometry of helix, the expressions for the changing geometric parameters are as follows:

$$\cos \beta = \frac{\pi N D}{L} \quad (21)$$

$$D = \frac{\sqrt{L^2 - H^2}}{N\pi} \quad (22)$$

The height of the actuator can be expressed in terms of the initial height and the deflection, as is shown in the next equation:

$$H = H_0 + \delta \quad (23)$$

Substituting β and D from the equations (21) and (22) into the equation (20) and integrating yield:

$$\delta = \frac{\partial U}{\partial F} = \left(\frac{F}{EA} \left(L - \frac{N^2}{L} (L^2 - H_0^2 - \delta^2 - 2H_0\delta) \right) + \left(\frac{F}{GA} + \frac{R^2 F}{GJ} \right) \left(\frac{N^2}{L} (L^2 - H_0^2 - \delta^2 - 2H_0\delta) \right) \right) \quad (24)$$

The above equation gives a polynomial of four degrees in terms of δ in the following form.

$$a_4\delta^4 + a_3\delta^3 + a_2\delta^2 + a_1\delta + a_0 = 0 \quad (25)$$

In low helix angles at which the sine of the angle approach to zero, the equation becomes the conventional linear load-displacement equation with a constant stiffness. In this study, the linear region of stiffness and low helix angles are focused. It is also supported by the fact that owing to significant elastic elongation, which is in contrary with thermal contraction, the actuator doesn't have a desirable performance in higher loads in terms of displacement.

3. Experiment and discussion

In this section, the simulation and experimental results for verifying the mathematical model are presented. The muscles were prepared according to our prior work [33], silver coated nylon of 200 μm diameter fiber was twisted and coiled from 500 mm long fiber, annealed and trained. The resulted muscle has a coiled diameter of 0.75 mm and a length of 150 mm. The TCP muscle actuated by a power supply using a well-controlled (controlled environment and disturbance) test stand. Temperature and displacement of the muscle were measured by a thermostat and a laser sensor, respectively. The muscle is fixed from one end and a weight is hung at the other. The experimental setup is shown in figure 6. It consists of a laser displacement sensor (Keyence LK-G152), a load cell (Futek LSB200), a power supply (BK Precision 1687B), type-E thermal couple and a National Instrument DAQ for data collection. The same experimental setup was used to generate experimental results for the TCP muscles in this paper [34, 35]. The tests were performed at four different step input current magnitude (0.18 A, 0.21 A, 0.24 A, and 0.27 A) and each test had 3 repeating cycles. The main objective of this work was to derive a model to predict the behavior of a TCP muscle and then verifying the model with an experiment. Therefore, we tried to obtain the most accurate measurement we could have by using the laser sensor and these measurement sensors were not intended to be a permanent part of the actuator in every application. The level of actuation is chosen according to the observed performance of the TCP muscle. The muscles start to move by a value near to the lowest actuation current and the neighboring coils come to contact with each other in a current value slightly higher than the highest actuation current. Therefore, we investigated 0.18–0.27 A actuation current. The number of repeating cycles is chosen to assure the repeatability of the tests. As it was observed, the TCP muscles show the same

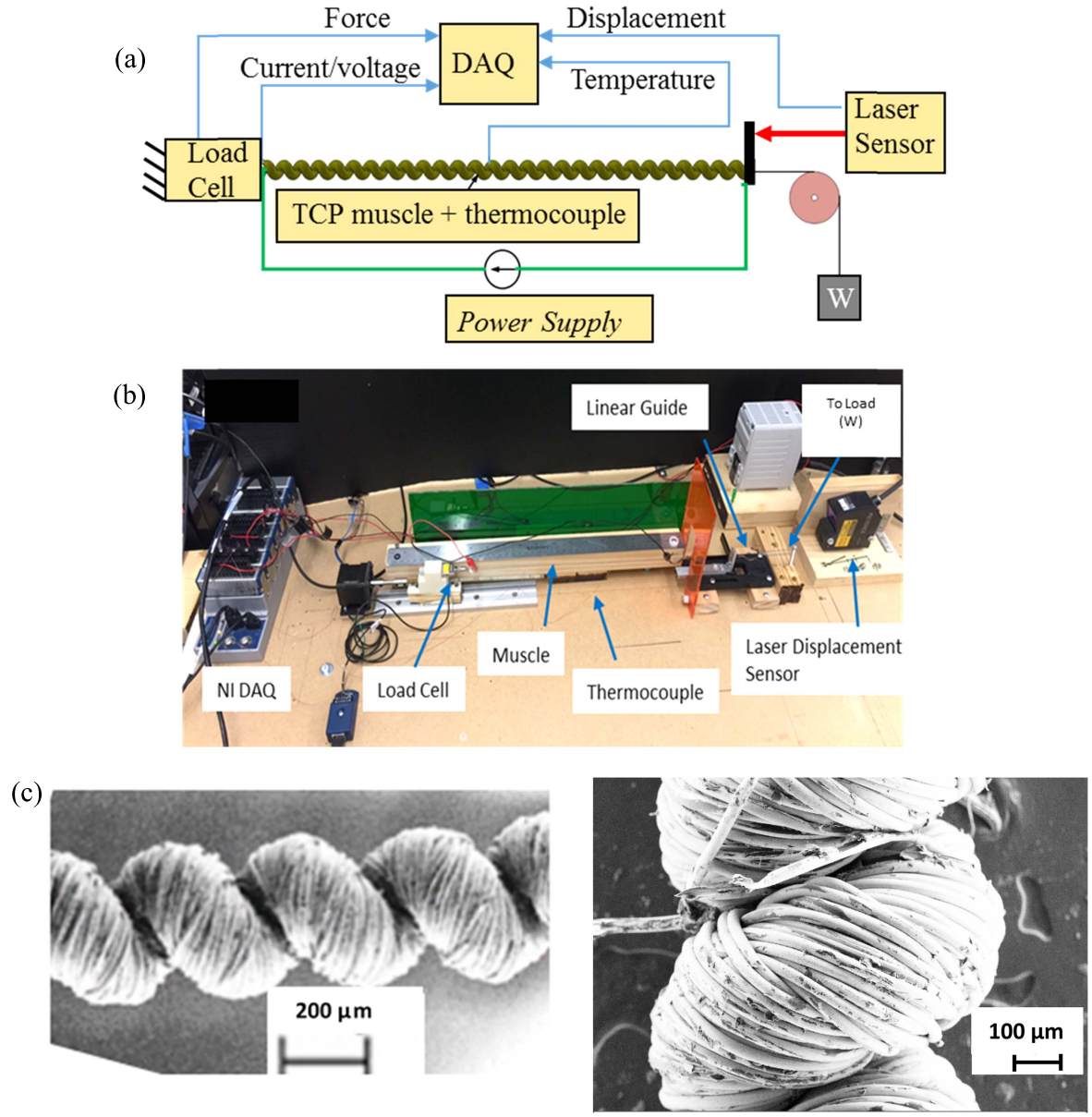

Figure 6. Experimental setup for TCP muscle characterization. (a) Schematic diagram, (b) the photograph of the setup and (c) SEM images of the 1-ply muscle.

behavior in the consecutive actuation cycles and go virtually the exact trajectory each time. For all tests, the actuation time was 25 s and the cooling time was 45 s, a period of total 75 s. The experimental data was stored for further analysis. Geometric parameters of the muscle, used in the test and simulation, are listed in table 1.

The CTE is adopted from [21], which was obtained from experiment for nylon 6,6 and the expression has the form of $\alpha_T = 1.35 \times 10^{-6}T + 4.2\ 10^{-4}$. We used this initial value and changed the coefficient to fit one of the displacement versus time plot and used it throughout the rest of the simulation. The longitudinal thermal expansion is expressed as:

$$\alpha(T) = -3.50 \times 10^{-6}T + 4.20 \times 10^{-4}\ K^{-1} \qquad (26)$$

Table 1. Parameters of the 1-ply TCP muscle used in the test.

Parameter	Symbol	Value	Reference
Initial Length	L_0	500 mm	Measurement
Initial Height	H_0	150 mm	Measurement
Initial Coil Diameter	D_0	0.75 mm	Measurement
Specific heat	c_p	1700 J kg^{-1} K	[36]
Mass	m	0.1 gram	Measurement
Stiffness at Room Temperature	k	23 N m^{-1}	Measurement
Resistance at Room Temperature	R_0	14 Ohm	Measurement
Ambient/Reference Temperature	T_0	23 °C	Measurement
Resistance Temperature Coefficient.	α	0.003 K^{-1}	[37]

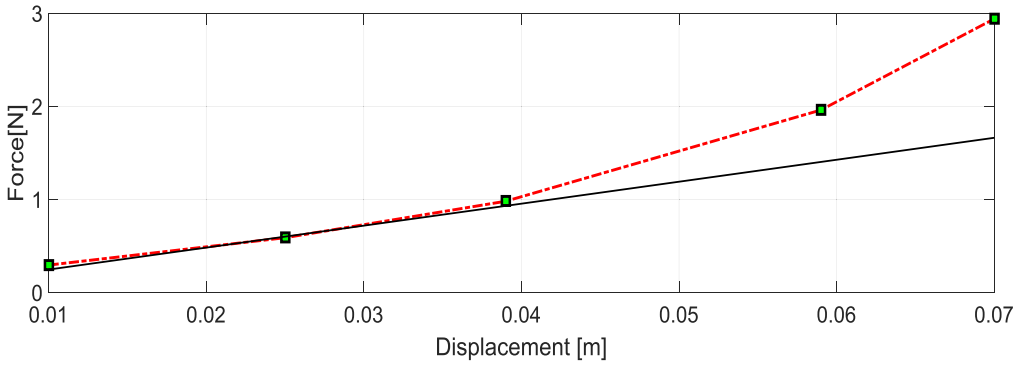

Figure 7. Displacement versus load in an isothermal experiment with the 1-ply TCP muscle of diameter 0.75 mm and initial length of 150 mm.

Where T is the temperature in Kelvin. A curve fitting to find elastic modulus versus temperature, based on the data of figure 3 is done. It leads to the following equation:

$$E(T) = -0.4655T^{1.381} + 536\,MPa \tag{27}$$

The material of TCP muscles affect the model through parameters and the way their electromechanical properties, such as their coefficient of thermal expansion and modulus of elasticity, and the change of these variables with temperature. They should be entered into the model for every other material, but there will be no change in the formulation of the mathematical relationship.

Another issue in the modeling of TCP muscles is the inductance due to the coiled geometry. The inductance can be determined by the standard solenoid equation:

$$L_H = k_p \mu \frac{N^2 A}{L} \tag{28}$$

Here $\boldsymbol{L_H}$ is the inductance of the actuator, N is the number of winding, A is the area, L is the length. $\mu = \mu_o k_p$, μ_o is the permeability of space ($4\pi \times 10{-}7\,\mathrm{T\,A{-}1\,m{-}1}$), and k_p is the relative permeability. Considering the tested TCP muscle (L = 150 mm, D = 0.75 mm, N = 280), the magnitude of the inductance value in the order of 10^{-6} H and this was ignored in this paper. However, this will be interesting to investigate in the future.

It is required to have the stiffness of the actuator at room temperature as a reference for calculating it in other temperatures. Generally, there are two methods for obtaining the stiffness. The first method is based on the geometric parameters together with appropriate assumptions on the mechanical model of the actuator. This method required a precise knowledge of the parameters, which are not easy to measure in general. The other is to conduct an isothermal load-displacement test at the room temperature, extracting the stiffness coefficient from the test result, and using it as a reference value. Figure 7 shows the load versus displacement for the TCP muscle using dead weight and measuring the displacement. There is a linear relationship between two quantities on the lower displacement (10–40 mm), which is associated with a low helix angle, but it deviates from the linear behavior as the load, and accordingly, the helix angle, increase. This result confirms the model proposed in the equation (25). At higher loads, due to the altering geometry from helical to straight form, the stiffness increases considerably and the total achievable displacement falls below the value of practical interest. According to the test results presented in figure 7, the linear relation is held up to 1N external load. In this work, the focus is on the linear response of the actuator, so its behavior beyond that limit is out of the scope of this work.

The first step for evaluating the proposed model is verifying its accuracy in predicting temperature, as the most influential factor on the behavior of the actuator. To quantify and validate the thermal model of TCP muscles, the test result of an actuation including heating and cooling periods was used. To assure the validity of the model, the coefficient of heat transfer was extracted from one of the test results. Due to high complexity in the geometry of the muscle, finding the exposed area would be a difficult task. Therefore, the value of convection heat transfer times exposed area (hA), instead of only convection coefficient (h), was identified. The hA value extracted from curve fittings, using the equation of heat transfer for cooling (equation (7)), was 0.15 with an error margin of 5% for all experimental data. This value was used for simulation of heating part. Figure 8 shows the simulation results and the test result for both heating and cooling cycle at different applied loads (30, 60 and 100 g) and current magnitudes(I = 0.18, 0.21, 0.24 and 0.27 A). As it is shown, the thermal model has a good accuracy and could follow the experimental data very well. The highest temperature was about 80 °C, corresponding to the highest actuation current magnitude. It is also observed that as the temperature rises, a slight divergence between the experimental and simulation result shows up. It is clear that the model predicts the temperature rise in the TCP muscle with a good accuracy for all its working linear range (for the electrical current magnitude of 0.18–0.24 A). It is worthy to note that for higher current levels (0.27 A), due to the excessive contraction of the muscle, the coils come to contact with each other and more displacement is prevented. Therefore, there should be a limit for actuation current in practical applications. This limit depends on the geometry and material of the muscle and also on the

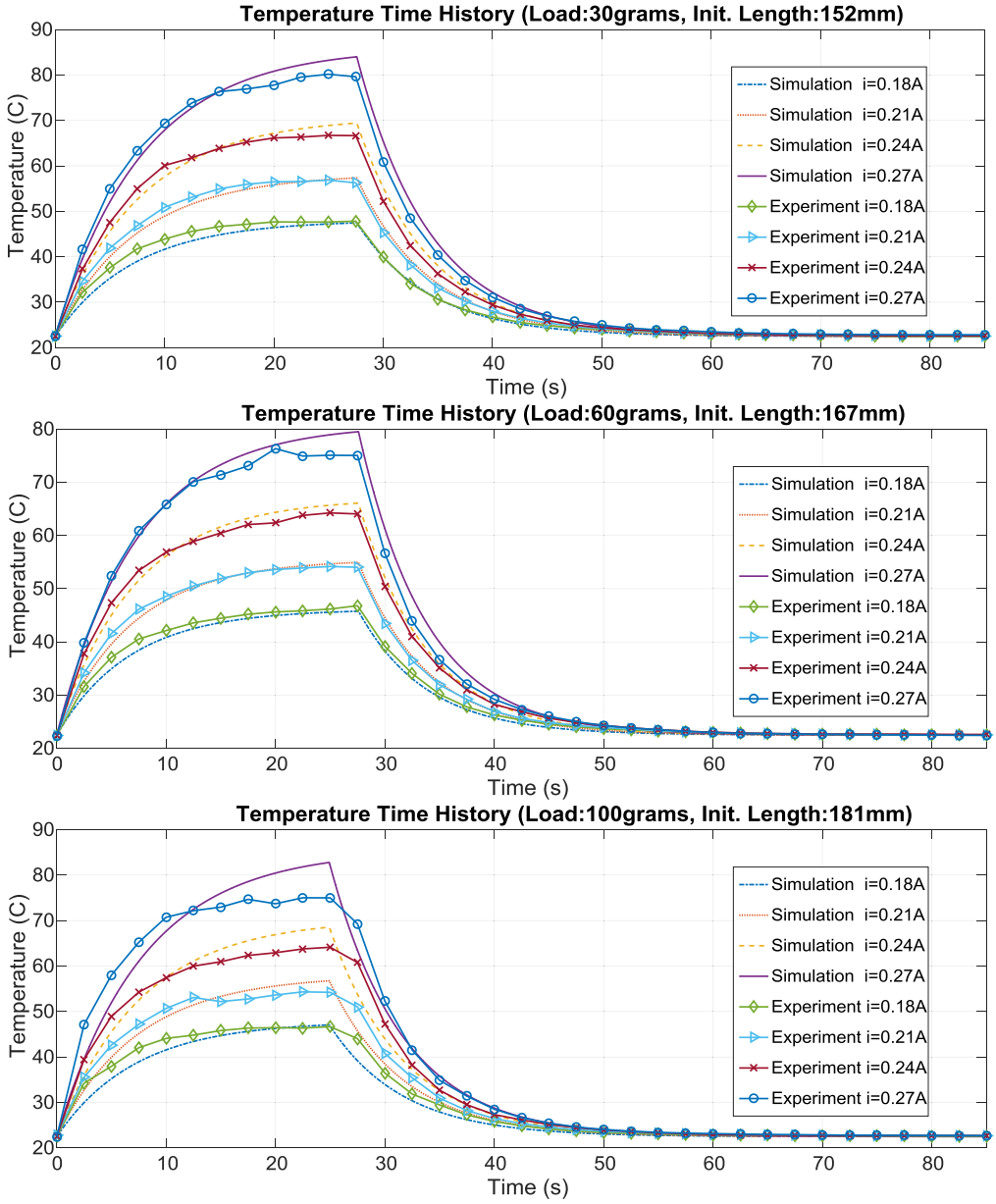

Figure 8. Simulation and experimental result of temperature in the TCP muscle during an actuation and cooling cycle for four actuation current levels and three load levels. Parameters of the muscles are as shown in table 1.

applied load. A temperature rise is needed to actuate, similar to shape memory alloy (SMA) actuators in order to have the phase transformation. In the case of SMA, the temperature change enables phase transformation from martensite to austenite and vice versa for actuation. Similarly, in TCPs, the temperature change (up to 80 °C with the input current of 0.27 A) causes the change of crystalline phase to rubber (amorphous) phase of the precursor polymer. This relatively high temperature will not be a major problem for this actuators compared to the numerous benefits as discussed before such as high actuation stroke, high energy density, and low cost.

The final analysis is dedicated to studying the displacement of the TCP muscle. The aim is to find the validity and accuracy of the model proposed for displacement of the muscle. The performance of the muscle is studied at three different load levels, the same as temperature study, and four current levels. The result of the simulation using equations (18) and (7) for the input temperature/current and the corresponding experimental results are shown in figure 9. As it is shown in the figure, the model exhibits accurate performance in predicting the dynamic displacement of the muscle for all studied current levels. In the heating cycle, where the displacement rises, the simulation result agrees with the experimental data; on the other hand, at the cooling phase, unlike the temperature simulation, there is a difference between two curves. Comparing temperature and displacement curve, there is some difference in the rising and falling part of the curve (after ~30 s) that makes the result deviate from the predicted value. For investigating this phenomenon, the experimental displacement versus temperature curve is plotted for one of the loads (30 grams) as shown in figure 10.

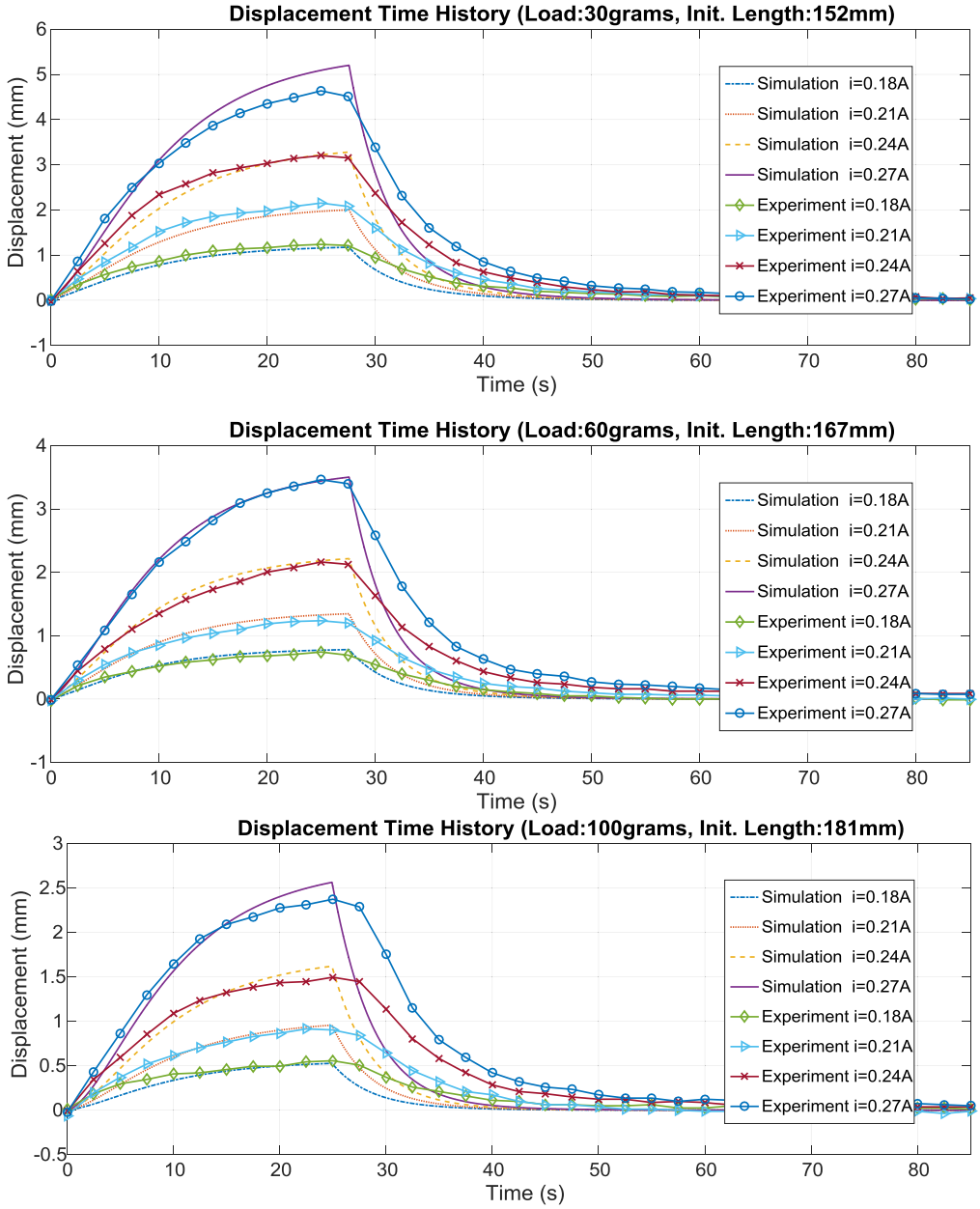

Figure 9. Simulation and experimental result of displacement in the TCP muscle during an actuation and cooling cycle for four actuation current levels and three load levels.

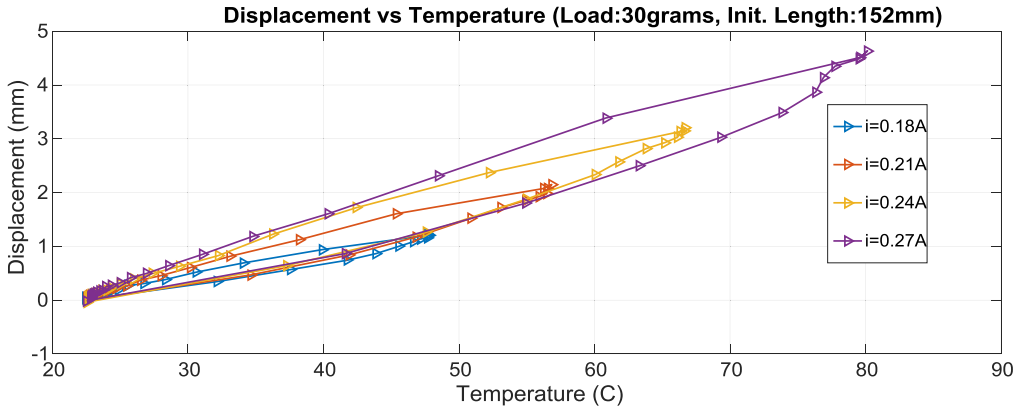

Figure 10. Experimental data of displacement versus temperature for 30 grams load and four different current levels of 1-ply TCP muscle.

As it is clear in figure 10, the muscle displacement goes different ways in cooling and heating phases. The top part of each curve corresponds to the heating and the bottom one to the cooling process and it repeats in successive actuation cycles for the same current level. There is a slight difference between the heating and cooling trajectories in the displacement-temperature plot. As the maximum temperature being raised, by increasing the actuation current, the difference grows. This phenomenon is more obvious at the temperatures above the glass transition temperature for the Nylon 6/6 which is around 50 °C. There is an active research on quantifying the hysteresis in twisted and coiled polymer actuators, and it was shown that generalized Prandtl-Ishlinskii model fits experimentally observed hysteresis [26]. It is to be noted that the hysteresis in TCPs is not as significant as shape memory alloy actuators as stated in Haines *et al* work [1]. In general, given that this phenomenon only shows up in the cooling phase, it has a little practical importance for the majority of applications.

4. Conclusion

In this paper, a practical electro-mechanical model is proposed for predicting the behavior of a TCP muscle actuated by Joule heating method. First, a differential equation of heat transfer is developed for predicting the temperature rise. The effect of a change in electrical resistance due to heating is also incorporated into the model and the simulations show a considerable contribution of this factor in the overall behavior. Second, the effect of temperature on the displacement of TCP muscles is modeled and quantified by modeling its effect on the length, through thermal expansion, and on the stiffness through changing the modulus of elasticity. The geometry of the muscle has also been found to have a considerable effect on the mechanical behavior. This effect is investigated and a comprehensive model including the helix angle of the muscle is derived. The outcome of this analysis is a nonlinear algebraic equation yielding the magnitude of displacement as a function of temperature and load. For verifying the obtained model, a set of simulations was done and results were compared with the experimental data. The model shows a good accuracy in predicting the temperature of muscles based on the electrical current magnitudes. Finally, the performance of the displacement model is investigated. The model exhibits very good accuracy in the heating phase for all the current and load levels. There is a difference between simulation and experimental results for displacement in the cooling phase which can be explained with the hysteresis theory but it needs further investigation. This model can be very useful for model-based control systems and robotics applications.

Acknowledgments

The authors would like to thank Lianjun Wu for providing experimental data. Yonas Tadesse would like to thank the Office of Naval Research (ONR) for the financial support, Young Investigator award under Grant N00014-15-1-2503.

ORCID iDs

Yonas Tadesse https://orcid.org/0000-0001-6606-7089

References

[1] Haines C S *et al* 2014 Artificial muscles from fishing line and sewing thread *Science* **343** 868–72
[2] Harris K D *et al* 2005 Large amplitude light-induced motion in high elastic modulus polymer actuators *J. Mater. Chem.* **15** 5043–8
[3] Choy C, Chen F and Young K 1981 Negative thermal expansion in oriented crystalline polymers *Journal of Polymer Science: Polymer Physics Edition* **19** 335–52
[4] Naficy S, Spinks G M and Baughman R H 2016 Bio-inspired polymer artificial muscles *Bio-inspired Polymers* (Royal Society of Chemistry) pp 429–59
[5] Haines C S, Li N, Spinks G M, Aliev A E, Di J and Baughman R H 2016 New twist on artificial muscles *Proc. of the National Academy of Sciences* p 201605273
[6] Wu L, de Andrade M J, Saharan L K, Rome R S, Baughman R H and Tadesse Y 2017 Compact and low-cost humanoid hand powered by nylon artificial muscles *Bioinsp. Biomim.* **12** 026004
[7] Saharan L, Sharma A, de Andrade M J, Baughman R H and Tadesse Y 2017 Design of a 3D printed lightweight orthotic device based on twisted and coiled polymer muscle: iGrab hand orthosis *Proc. SPIE* **10164** 1016428
[8] Almubarak Y and Tadesse Y 2017 Design and motion control of bioinspired humanoid robot head from servo motors toward artificial muscles *Proc. SPIE* **10163** 101631U
[9] Almubarak Y and Tadesse Y Twisted and coiled polymer (TCP) muscles embedded in silicone elastomer for use in soft robot *Int. Journal of Intelligent Robotics and Applications* **1** 352–68
[10] Tomar A and Tadesse Y 2016 Multi-layer robot skin with embedded sensors and muscles *Proc. SPIE* **9798** 979809
[11] Wu L, de Andrade M J, Brahme T, Tadesse Y and Baughman R H 2016 A reconfigurable robot with tensegrity structure using nylon artificial muscles *Proc. SPIE* **9799** 97993K
[12] Saharan L, de Andrade M J, Saleem W, Baughman R H and Tadesse Y 2017 iGrab: hand orthosis powered by twisted and coiled polymer muscles *Smart Mater. Struct.* **26** 105048
[13] Arjun A, Saharan L and Tadesse Y 2016 Design of a 3D printed hand prosthesis actuated by nylon 6-6 polymer based artificial muscles *Automation Science and Engineering (CASE), 2016 IEEE Int. Conf. on* pp 910–5
[14] Tadesse Y, Wu L and Saharan L K 2016 Musculoskeletal system for bio-inspired robotic systems *Mech. Eng.* **138** S11
[15] Wu L and Tadesse Y 2016 Musculoskeletal system for bio-inspired robotic systems based on ball and socket joints *ASME 2016 Int. Mechanical Engineering Congress and Exposition* (American Society of Mechanical Engineers) pp V04AT05A020
[16] Liang C and Rogers C 1993 Design of shape memory alloy springs with applications in vibration control *Journal of Vibration and Acoustics* **115** 129–35
[17] Tadesse Y, Villanueva A, Haines C, Novitski D, Baughman R and Priya S 2012 Hydrogen-fuel-powered bell segments of biomimetic jellyfish *Smart Mater. Struct.* **21** 045013
[18] Yang Q and Li G 2016 Temperature and rate dependent thermomechanical modeling of shape memory polymers with physics based phase evolution law *Int. Journal of Plasticity* **80** 168–86
[19] Varghese A and Batra R 2009 Constitutive equations for thermomechanical deformations of glassy polymers *Int. Journal of Solids and Structures* **46** 4079–94

[20] Yip M C and Niemeyer G 2017 On the control and properties of supercoiled polymer artificial muscles *IEEE Transactions on Robotics* **33** 689–99
[21] Yang Q and Li G 2016 A top-down multi-scale modeling for actuation response of polymeric artificial muscles *Journal of the Mechanics and Physics of Solids* **92** 237–59
[22] Sharafi S and Li G 2015 A multiscale approach for modeling actuation response of polymeric artificial muscles *Soft Matter* **11** 3833–43
[23] Shafer M W, Feigenbaum H P, Pugh D and Fisher M 2016 First steps in modeling thermal actuation of twisted polymer actuators using virgin material properties *ASME 2016 Conf. on Smart Materials, Adaptive Structures and Intelligent Systems* (American Society of Mechanical Engineers) pp V002T06A017
[24] van der Weijde J, Smit B, Fritschi M, van de Kamp C and Vallery H 2016 Self-sensing of displacement, force and temperature for joule-heated twisted and coiled polymer muscles via electrical impedance *IEEE/ASME Trans. Mechatronics* **22** 1268–75
[25] Arakawa T, Takagi K, Tahara K and Asaka K 2016 Position control of fishing line artificial muscles (coiled polymer actuators) from nylon thread *Proc. SPIE* **9798** 97982W
[26] Zhang J, Iyer K, Simeonov A and Yip M C 2017 Modeling and inverse compensation of hysteresis in supercoiled polymer artificial muscles *IEEE Robotics and Automation Letters* **2** 773–80
[27] Boetcher S K 2014 *Natural Convection from Circular Cylinders* (Berlin: Springer) (https://doi.org/10.1007/978-3-319-08132-8)
[28] Saharan L and Tadesse Y 2016 Fabrication parameters and performance relationship of twisted and coiled polymer muscles *ASME 2016 Int. Mechanical Engineering Congress and Exposition* (American Society of Mechanical Engineers) pp V014T11A028
[29] Tadesse Y, Thayer N and Priya S 2010 Tailoring the response time of shape memory alloy wires through active cooling and pre-stress *Journal of Intelligent Material Systems and Structures* **21** 19–40
[30] Tadesse Y, Hong D and Priya S 2011 Twelve degree of freedom baby humanoid head using shape memory alloy actuators *Journal of Mechanisms and Robotics* **3** 011008
[31] Saharan L, Andrade M J D, Saleem W, Baughman R H and Tadesse Y 2017 iGrab: hand orthosis powered by twisted and coiled polymer muscles *Smart Mater. Struct.* **26** 105048
[32] Beer F P, Johnston R, Dewolf J and Mazurek D 1981 Mechanics of Materials (New York: McGraw-Hill) pp 150–233
[33] Wu L *et al* 2017 Compact and low-cost humanoid hand powered by nylon artificial muscles *Bioinspiration & Biomimetics* **12** 026004
[34] Jafarzadeh M, Wu L and Tadesse Y 2017 System identification of force of a silver coated twisted and coiled polymer muscle *IMECE 2017* Tampa, Florida, vol. IMECE2017-71985: ASME
[35] Wu L and Tadesse Y 2017 Modeling of the electrical resistance of TCP muscle *IMECE 2017* Tampa, Florida, vol. IMECE2017-72065: ASME
[36] Mark J E 2007 *Physical Properties of Polymers Handbook* (Berlin: Springer) (https://doi.org/10.1007/978-0-387-69002-5)
[37] David J G 1999 *Introduction to Electrodynamics* (Delhi: Prentice Hall) (https://doi.org/10.1201/b15442-4)